



This is the accepted manuscript made available via CHORUS, the article has been published as:

High-Pressure Core Structures of Si Nanoparticles for Solar Energy Conversion

S. Wippermann, M. Vörös, D. Rocca, A. Gali, G. Zimanyi, and G. Galli

Phys. Rev. Lett. **110**, 046804 — Published 24 January 2013

DOI: [10.1103/PhysRevLett.110.046804](https://doi.org/10.1103/PhysRevLett.110.046804)

High pressure core structures of Si nanoparticles for solar energy conversion

S. Wippermann^{1,2}, M. Vörös³, D. Rocca¹, A. Gali^{3,4}, G. Zimanyi² and G. Galli^{1,2}

¹*Department of Chemistry, University of California, Davis, California 95616, USA*

²*Department of Physics, University of California, Davis, California 95616, USA*

³*Department of Atomic Physics, Budapest University of Technology and Economics, Budafoki út 8, H-1111 Budapest, Hungary*

⁴*Institute for Solid State Physics and Optics, Wigner Research Center for Physics, Hungarian Academy of Sciences, Budapest, PO Box 49, H-1525, Hungary*

(Dated: November 2, 2012)

We present density functional and many body perturbation theory calculations of the electronic, optical and impact ionization properties of Si nanoparticles (NPs) with core structures based on high pressure bulk Si phases. Si particles with a BC8 core structure exhibit significantly lower optical gaps and multiple exciton generation (MEG) thresholds, and an order of magnitude higher MEG rate than diamond-like ones of the same size. Several mechanisms are discussed to further reduce the gap, including surface reconstruction and chemistry, excitonic effects, and embedding pressure. Experiments reported the formation of BC8 NPs embedded in amorphous Si and in amorphous regions of femtosecond-laser doped “black silicon”. For all these reasons, BC8 nanoparticles may be promising candidates for MEG-based solar energy conversion.

PACS numbers: 73.22.-f, 61.46.Hk, 71.35.-y

Third generation solar cell designs aspire to transcend the Shockley-Queisser (SQ) limit of 33.7 % for the efficiency of solar energy conversion by employing path breaking new paradigms. Multiple Exciton Generation (MEG) is one of these new paradigms, where an incoming photon generates a high energy exciton, which then decays into multiple excitons. While the efficiency of MEG in bulk semiconductors is small, in 2002 Nozik suggested that in nanoparticles (NPs) the effective Coulomb interaction is enhanced by quantum confinement and the electronic screening decreased, driving the efficiency of MEG to promisingly high values [1]. In 2004-2006, the Klimov group demonstrated that a strong MEG may indeed be obtained in semi-conducting NPs (e. g. [2]), triggering intense theoretical and experimental interest [3–11]. While the efficiency enhancement reported in Ref. [2] was later questioned [3], the presence of MEG was eventually verified in colloidal NPs, albeit with a reduced magnitude [6]. Recently, Semonin et al. demonstrated that the excess electrons generated by the MEG can be efficiently extracted from the NPs to the electrodes of a functioning PbSe NP solar cell; the MEG enhanced the external quantum efficiency above 100% within a region of the solar spectrum [12].

The remaining challenges include the high energy threshold required to activate the MEG, estimated theoretically to be twice the optical gap but found experimentally around thrice the gap. Therefore, the solar photons can be best captured by multiple exciton generation in materials with gaps in the 0.5-1.0 eV range [13]. Moreover, for concentrated solar cells with a concentration factor of 500, the optimal gap has been shown to be as low as 0.1 eV [14].

At the nanoscale, the quantum confinement enhances the Coulomb interaction, thereby allowing for efficient MEG [1], but it also increases the gap and reduces the density of states (DOS) at any given energy. The increase

of the gap with decreasing NP radius can swiftly shift the MEG threshold energy outside the solar spectrum. On the other hand, lowering the gap may reduce the effective Coulomb interaction and thus MEG efficiency. Therefore, two competing requirements have to be satisfied by identifying semiconducting NPs featuring simultaneously (i) a small excitation gap and a DOS only moderately reduced with respect to the bulk, and (ii) efficient MEG despite suitably small gaps. We note that MEG efficiency is often measured on a relative energy scale, in units of the gap, to compare systems with different gaps; however the utility of MEG for solar application has ultimately to be established on an absolute energy scale.

In this Letter we present density functional theory (DFT) and many body perturbation theory (MBPT) calculations of the electronic, optical and impact ionization

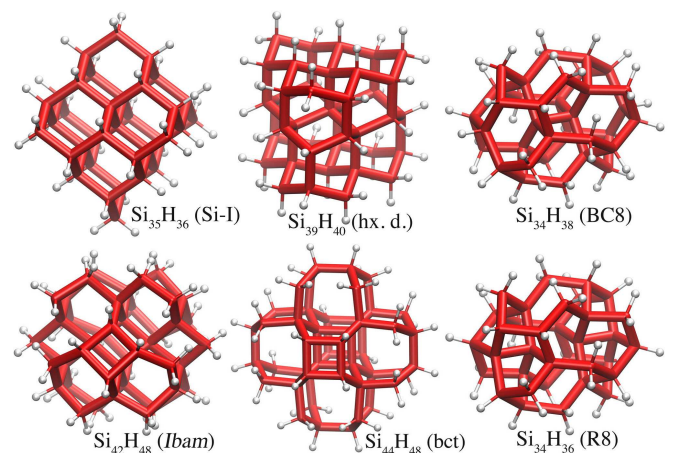


FIG. 1: (color online). Structural models of ~ 1 nm hydrogenated Si NPs with Si-I, Si-IV (hexagonal diamond), Si-XII (R8), Si-III (BC8), *Ibam* and *bct* core structures.

properties of hydrogenated Si NPs with core structures resembling those of high pressure Si phases. We show that these nanoparticles, especially those with the BC8 structure, exhibit simultaneously (i) low optical absorption thresholds, and (ii) enhanced MEG rates even on an absolute energy scale. Hence we propose these systems are promising candidates for MEG based solar energy conversion.

To put our work into context, we recall that bulk Si retains its cubic diamond (Si-I or cd) structure upon compression up to ~ 11.7 GPa, while its optical gap is reduced. Above ~ 11.7 GPa, Si-I transforms to the metallic β -tin phase (Si-II) which, upon pressure (P) release does not revert back to Si-I, but transforms into a series of metastable high-density phases with distorted tetrahedral bonding [15]. Under slow P release, Si-XII/R8 is detected at ~ 8 GPa, followed by a transition to Si-III/BC8. Subsequent annealing at moderate temperatures leads to the formation of hexagonal diamond (Si-IV/hd) [15, 16]. If β -tin is decompressed rapidly (< 100 ms), two additional phases may be observed, Si-VIII and Si-IX, for which only incomplete structural information is available. It has been recently proposed that Si-IX has the *Ibam* structure [17]. Finally, two other Si polymorphs were predicted theoretically but not yet observed experimentally, ST12 [18] and bct [19].

In 2006, Arguirov *et al.* reported the formation of BC8 Si NPs within amorphous Si in a-Si/SiO₂ multilayer stacks [20]. In addition Smith *et al.* [21] showed that R8 and BC8 NPs are formed when “black silicon” is produced by irradiating highly doped Si surfaces with femtosecond laser pulses. The authors argued that pressure waves generated by the fs-pulses first amorphized regions of the sample and then induced the nucleation of R8 and BC8 NPs within these regions. Importantly, in the regions of the sample where BC8 NPs were detected, the absorption was substantially enhanced, especially at sub-gap energies, and then decreased upon annealing of the NPs. This suggests that BC8 particles played an active role in enhancing the low energy absorption. Formation of nanocrystalline BC8 regions were also observed in nano-grinding experiments [22] and in SiGe epilayers [23].

These experiments suggest that Si NPs with core structures based on high pressure Si phases are promising candidates to exhibit a lower gap than Si-I NPs and low energy optical absorption, especially the BC8 phase, which is gapless in the bulk. However, a detailed analysis it required to establish whether the strength of the Coulomb interaction is preserved and whether efficient MEG is still present in such Si NPs.

To explore the possible advantages of Si NPs with high pressure core structures, we carried out electronic structure calculations within DFT and MBPT. We used the local density approximation (LDA) [24] and norm-conserving pseudopotentials [25] with an energy cutoff of 35 Ry, and the QUANTUM ESPRESSO package [26]. Quasiparticle energies within the GW scheme [27] were

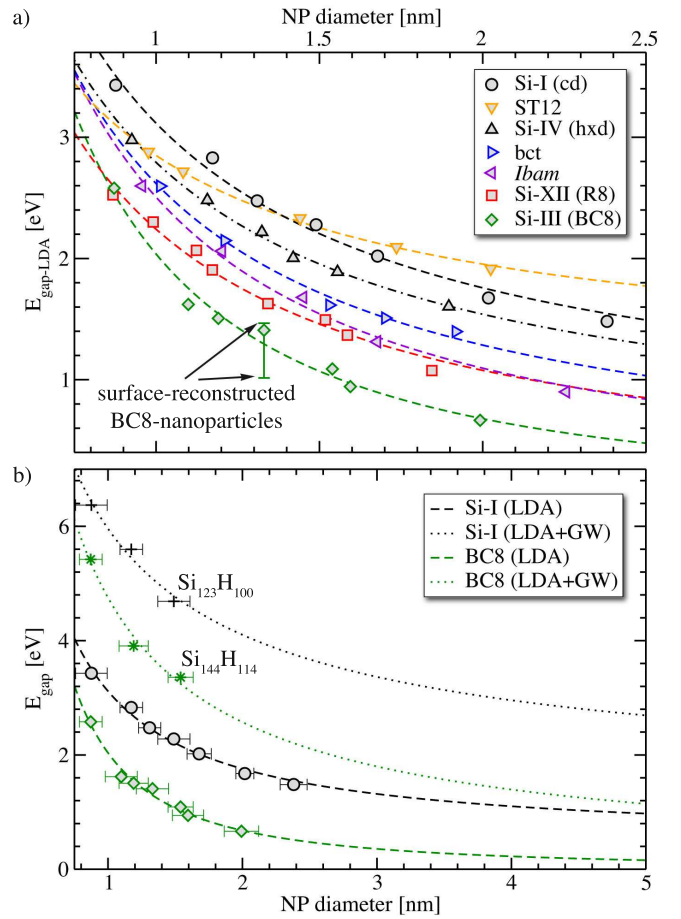


FIG. 2: (color online). Electronic gaps of hydrogenated Si nanocrystals as a function of the nanoparticle (NP) diameter computed using a) the Local Density Approximation (LDA) and b) many body perturbation theory within the GW approximation (GW). Symbols and lines refer to calculated values and fits (cf. Tab. I), respectively. Sizes are given as twice the average radial distance of the NP surface atoms to the NP center, with size error bars representing the standard deviation. The core structures of the NPs are labeled in the inset according to the nomenclature used for tetrahedrally bonded bulk Si phases (see text).

obtained employing the approach of Nguyen *et al.*, which avoids the explicit calculation of empty electronic states and the inversion of large dielectric matrices [28]. Optical absorption spectra were calculated within time-dependent density functional theory (TDDFT), using the LDA and random phase approximation (RPA) and the Liouville-Lanczos approach [29, 30]. Based on the results of our previous study [31] and the findings of Ref. [32, 33] we assumed that the major contribution to MEG comes from impact ionization (II) processes and we approximated MEG rates with II rates. We used the Fermi Golden Rule to obtain the decay rate of excitons to bi-excitons. The initial exciton and final bi-exciton states were approximated as singly and doubly excited Slater-determinants, built up from DFT orbitals [31] in the gen-

PHASE	$E_{g,NP}$ [eV] (GW)					fitting constants		
	0.9nm	1.2nm	1.5nm	4nm	8nm	E_g [eV]	a [eV]	b
cd	6.37	5.60	4.69	2.95	2.24	1.12	4.84	0.70
BC8	5.42	3.91	3.35	1.37	0.74	0.00	4.75	0.88
hd	5.89	5.16				0.95		
<i>Ibam</i>	5.24	4.51				0.24		
R8	4.96	4.37				0.24		
bct	5.35	4.94				1.54		
ST12	5.57	5.30				1.54		

TABLE I: Electronic gaps of nanoparticles ($E_{g,NP}$) and bulk phases (E_g) obtained using the GW approximation. GW bulk gaps are taken from Refs. [15, 50, 51]. $E_{g,NP}$ were computed for particles up to ~ 1.5 nm in GW (see Fig. 2) and extrapolated to 4 nm and 8 nm using the relation $E_{g,NP} = E_{g,bulk} + a \cdot ([nm]/d)^b$, where d is the NP diameter and a , b are fitting constants. The high pressure Si phases (left column) are defined in the text.

eralized gradient approximation (GGA) [34]. To account for the dielectric screening within our GW and II calculations we computed the dielectric matrix within the random phase approximation (RPA) using iterative techniques [35].

The core geometry of the Si NPs was built by isolating a sphere of a given radius from the structure of the respective Si bulk phases. The radius and center of this sphere were chosen so as to obtain NPs with no more than two dangling bonds per surface atom. All dangling bonds were saturated with hydrogen atoms. The whole structure was then allowed to relax to the nearest local energy minimum. Fig. 1 shows the resulting final geometries of Si NPs for a diameter of ~ 1 nm.

In all NPs we found almost bulk-like bond lengths and angles near the core. In proximity of the surface the bond lengths contract and the angular distribution is slightly broadened in comparison with the corresponding one in the bulk. Overall, Si-I NPs exhibit a bond length deviation of $(-0.16 \pm 0.24)\%$, whereas the structures based on other tetrahedrally bonded phases exhibit larger deviations, e. g. $(-0.22 \pm 0.80)\%$ for BC8 NPs [36].

The electronic gap of NPs with various core structures as a function of size is shown in Fig. 2 and Tab. I. Sizes are given as twice the average radial distance of the NP surface atoms to the center, with size error bars representing the corresponding standard deviation. The BC8 NPs have significantly smaller gaps than all the other nanoparticles. For example, at the LDA level the gap of a BC8 NP of diameter 2.5 nm is 1 eV lower than that of Si-I NPs of the same size. This substantial difference is consistent with the fact that BC8 is a semi-metal in the bulk. In fact, recent quasiparticle calculations for bulk BC8 predicted a 0.44 eV direct overlap of the bands at the H point [15], while measurements suggested an indirect overlap of 0.3 eV [37]. Our result is also in agreement with earlier empirical tight binding calculations [38].

Given the tendency of local DFT calculations to un-

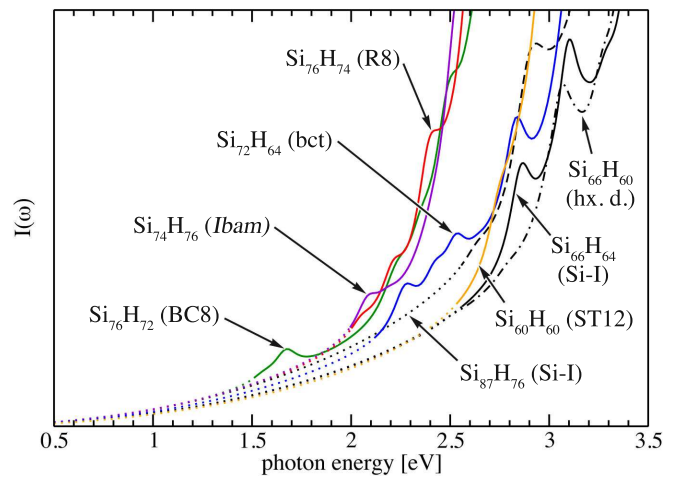


FIG. 3: (color online). Optical absorption spectra of 1.2 nm NPs computed using time dependent density functional theory. The spectrum of a Si-I 1.3 nm NP ($\text{Si}_{87}\text{H}_{76}$) is included for comparison. A broadening of 0.005 Ry was used. Dotted lines indicate low energy features induced by the broadening.

derestimate band gaps, we performed quasiparticle calculations in the GW approximation for NP diameters up to 1.2 nm (~ 76 Si atoms), to assess the validity of the trends observed within LDA. As expected, all computed GW gaps are larger than the LDA ones; however the same trends as a function of the NP diameter were found at both levels of theory (see Table I) [39].

Both LDA and GW energy gaps for larger nanoparticles were estimated by fitting the calculated NP and bulk gaps by a power law. The fits are reported in Tab. I and Fig. 2. At 2.5 (8.0) nm, the Si-I GW gaps are 3.6 (2.2) eV and those of BC8 are 2.1 (0.7) eV. We emphasize that at the experimentally accessible diameter of 4 nm to 8 nm the GW gap of BC8 NPs is 1.4 eV to 0.7 eV, near optimal for solar applications.

The quasi particle gaps obtained here are an upper bound to optical gaps, as excitonic effects are not taken into account [40, 41] and they may be expected to be larger than in the bulk, as suggested by QMC calculations [42]. In addition, several other factors contribute to lowering the quasi particle gaps, including surface reconstruction, symmetry breaking, pressure effects and finite T geometrical distortions. To estimate the magnitude of these effects, we calculated the gaps of surface reconstructed 1.35 nm BC8 NPs for all possible permutations of surface bonds, generated by rearranging the available twofold coordinated surface Si-atoms. The distribution of the calculated gap values extended 0.5 eV lower than that of the gap of the ideally terminated NP. The width of the distribution is indicated by the bar in Fig. 2a.

Residual compressive stress can also reduce the gap, e.g., in the case of R8 and BC8 NPs embedded in a matrix, as suggested by Smith *et al.* [21] on the basis of Raman spectra analysis. In addition, the gap may be affected by the chemical composition of the NP-matrix

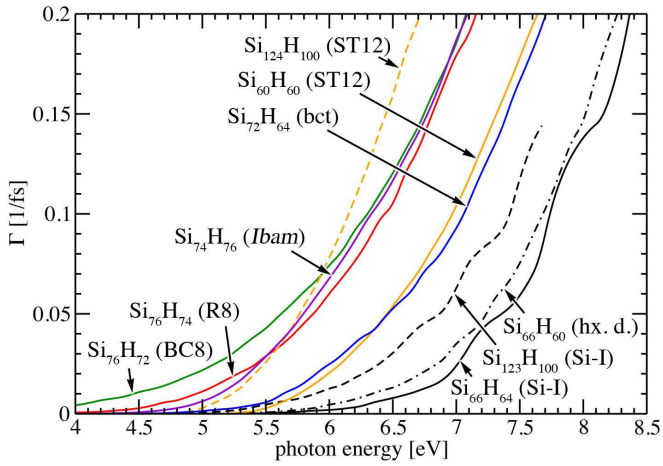


FIG. 4: (color online). Impact ionization rates for ~ 1.2 nm sized NPs on the absolute energy scale. Note that compared to Fig. 3 the energy scale has been shifted to highlight the threshold region of MEG.

interface, especially for small diameters ($d < 4$ nm). For example, Si-I NPs embedded in amorphous silica exhibit a gap reduced by more than 1 eV compared to that of NPs embedded in Si_3N_4 or hydrogenated ones [43]. The difference increases with decreasing NP size. Similar effects were found for Si NPs embedded in ZnS [44, 45].

To investigate whether the reduced gaps in NPs with high pressure core-like structures correspond to optically active transitions and result in a red-shifted optical absorption spectrum, compared to that of Si-I NPs, we calculated the optical response at the TDDFT-RPA level. Fig. 3 shows the optical absorption spectra of ~ 1.2 nm NPs. On average, in the interval 2 to 5 eV, the spectra of Si-I and BC8 NPs are shifted by 0.5 eV. This shift is smaller than the electronic gap difference, as the matrix element for the BC8 HOMO/LUMO transition is smaller than that of the Si-I NP.

As discussed earlier, in NPs the quantum confinement enhances the Coulomb interaction, but it also increases the gap, reducing the DOS. On the other hand, lowering the gap may weaken the Coulomb interaction and thus MEG. Therefore, to explore whether these low-gap core structures feature reduced or enhanced MEG compared to Si-I NPs, we calculated the impact ionization (II) rates of the initial photo-excited excitons decaying into bi-excitons using the Fermi Golden Rule. Fig. 4 shows the II rate $\Gamma(E)$ on an absolute energy scale for NPs with diameter ~ 1.2 nm. The figure shows that the NPs with high pressure core structures feature efficient MEG despite smaller gaps; for example the BC8 gap being smaller than the Si-I one by 1.3 eV leads to its $\Gamma(E)$ II rate to be red shifted by 2.0 eV relative to Si-I. This redshift translates to the MEG of BC8 NPs being about an order of magnitude larger than for diamond-like NPs at energies close to the onset of MEG.

Finally, we investigated MEG in the hypothetical ST12 structure, proposed theoretically for bulk Si [18] and

observed experimentally for Ge [46]. This structure is notably different from the other tetrahedrally bonded phases, as its gap is larger than that of Si-I (see Fig. 2 and Tab. I). However, the ST12 NPs exhibit enhanced DOS just above the gap to significantly higher values than the other NPs. Fig. 4 shows that with increasing size the II rate for the ST12 NPs is increased much faster than for the Si-I NPs. While increasing size and thus decreasing quantum confinement make the effective Coulomb interaction weaker and thus undermine the efficiency of MEG, the large DOS of ST12 at lower energies restores the MEG efficiency. Although ST12 is still a hypothetical phase of Si, stable Ge NPs with ST12 structures have already been obtained in a wide range of sizes [47], and are surprisingly stable, up to 500 °C at ambient pressure. Earlier DFT calculations indicated that amorphous shells around Ge nanocrystals can induce sufficient pressure to stabilize the Ge core structure within the ST12 phase [48]. Since the gaps of Ge NPs are expected to be lower than those of Si, and since Ge is known to exhibit carrier multiplication in the bulk [6], Ge NPs in general, and their ST12 phase in particular are promising candidates for utilizing MEG for solar energy conversion.

In summary, we calculated the electronic and optical properties and the impact ionization rates of Si nanoparticles with core structures based on high pressure Si bulk phases. We used several levels of theory including DFT-LDA, TDDFT-RPA and MBPT at the GW level. We found that BC8 like NPs exhibited significantly lower electronic gaps and a red shifted optical absorption, compared to diamond-like ones. Importantly, they also showed an enhanced MEG efficiency, contrary to the expectation that lowering the gap may lead to reduced MEG efficiency, because of the reduced effective Coulomb interaction. Several additional factors were explored that can further lower the NPs gap and further enhance the efficiency of MEG, including surface reconstruction, residual compressive stress from matrix-embedding, and chemical shifts caused by chalcogens at the NP-matrix interface. An optical gap lower than in diamond-like particles is a highly desirable feature not only for MEG-based solar cells but also for long wavelength absorber layers in all-Si NP tandem cells [49]. Tantalizingly, recent experiments have shown that it is possible to form Si NPs with BC8 core structures in amorphous Si samples under high compressive strain conditions [20, 21]. Overall, our findings suggest that creating MEG-based photovoltaic cells with high pressure Si core like structures (and possibly Ge) may be a promising paradigm for solar energy conversion.

The authors wish to thank G. Crabtree, V. Klimov, A. Nozik, A. Zunger, O. Semonin and T. A. Pham for helpful discussions. This research was supported by the NSF-Solar Collaborative (No. DMR-1035468), DOE/BES (Contract No. DE-FG02-06ER46262) and the Deutsche Forschungsgemeinschaft (Grant No. WI3879/1), as well as supercomputer time provided by NERSC (NISE-

35687) and the ShaRCS Pilot Project.

-
- [1] A. J. Nozik, *Physica E* **14**, 115 (2002)
- [2] R. D. Schaller *et al.*, *Phys. Rev. Lett.* **92**, 186601 (2004)
- [3] G. Nair, M. G. Bawendi, *Phys. Rev. B* **76**, 081304 (2007)
- [4] J.-W. Luo *et al.*, *Nano Letters* **8**, 3174 (2008)
- [5] M. C. Beard *et al.*, *Nano Letters* **7**, 2506 (2007)
- [6] M. C. Beard, *J. Phys. Chem. Lett.* **2**, 1282 (2011)
- [7] D. Timmerman *et al.*, *Nature Photon.* **2**, 105 (2008)
- [8] D. Timmerman *et al.*, *Nature Nanotech.* **6**, 710 (2011)
- [9] W. A. Su *et al.*, *Appl. Phys. Lett.* **100**, 071111 (2012)
- [10] M. T. Trinh *et al.*, *Nature Photon.* **6**, 316 (2012)
- [11] M. C. Beard *et al.*, *Acc. Chem. Res.* (2012)
- [12] O. E. Semonin *et al.*, *Science* **334**, 1530 (2011)
- [13] M. Hanna, A. Nozik, *J. Appl. Phys.* **100**, 074510 (2006)
- [14] A. Nozik, private communication
- [15] B. Malone *et al.*, *Phys. Rev. B* **78**, 035210 (2008)
- [16] M. Cohen, B. Malone, *J. Appl. Phys.* **109**, 102402 (2011)
- [17] B. Malone, M. Cohen, *Phys. Rev. B* **85**, 024116 (2012)
- [18] S. J. Clark *et al.*, *Phys. Rev. B* **49**, 5341 (1994)
- [19] Y. Fujimoto *et al.*, *N. J. Phys.* **10**, 083001 (2008)
- [20] T. Arguirov *et al.*, *Appl. Phys. Lett.* **89**, 053111 (2006)
- [21] M. J. Smith *et al.*, *J. Appl. Phys.* **110**, 053524 (2011)
- [22] Y. Wang *et al.*, *Nanotechnology* **18**, 465705 (2007)
- [23] M. Pandey *et al.*, *J. Phys. Cond. Mat.* **20**, 335234 (2008)
- [24] J. Perdew, A. Zunger, *Phys. Rev. B* **23**, 5048–5079 (1981)
- [25] D. Hamann *et al.*, *Phys. Rev. Lett.* **43**, 1494 (1979)
- [26] P. Giannozzi *et al.*, *J. Phys. Cond. Mat.* **21**, 395502 (2009)
- [27] L. Hedin, *Phys. Rev.* **139**, A796 (1965)
- [28] H.-V. Nguyen *et al.*, *Phys. Rev. B* **85**, 081101 (2012)
- [29] D. Rocca *et al.*, *J. Chem. Phys.* **128**, 154105 (2008)
- [30] O. B. Malcioglu *et al.*, *Comp. Phys. Comm.* **182**, 1744 (2011)
- [31] M. Vörös *et al.*, (to be published)
- [32] A. Piryatinski *et al.*, *J. Chem. Phys.* **133**, 084508 (2010)
- [33] K. Velizhanin *et al.*, *Phys. Rev. Lett.* **106**, 207401 (2011)
- [34] J. Perdew, K. Burke, M. Ernzerhof, *Phys. Rev. Lett.* **77**, 3865 (1996)
- [35] H. Wilson *et al.*, *Phys. Rev. B* **78**, 113303 (2008), H. Wilson *et al.*, *Phys. Rev. B* **79**, 245106 (2009)
- [36] Compared to bulk Si-I, cd, hd and bct NPs show only small deviations from both the Si-I bulk bond length and angle. ST12 and *Ibam* exhibit by far the largest deviations and also variances, closely followed by R8. BC8 shows intermediate deviations but the largest variance of all phases in terms of bond lengths by $(0.35 \pm 1.24)\%$. However, with $(-1.17 \pm 8.45)\%$ the angles scatter less than for R8, *Ibam* and ST12.
- [37] J. M. Besson *et al.*, *Phys. Rev. Lett.* **59**, 473 (1987)
- [38] C. Delerue *et al.*, *J. Luminescence* **80**, 65 (1999)
- [39] We verified that the GW energy levels showed no inversion relative to the LDA levels for 80 empty states, spanning an energy range of 3.3 eV.
- [40] C. Delerue *et al.*, *Phys. Rev. Lett.* **84**, 2457 (2000)
- [41] A. R. Porter *et al.*, *Phys. Rev. B* **64**, 035320 (2001)
- [42] A. Williamson *et al.*, *Phys. Rev. Lett.* **89**, 196803 (2002)
- [43] G. Conibeer *et al.*, *Thin Solid Films* **516**, 6748 (2008)
- [44] S. Wippermann *et al.*, (to be published)
- [45] We note that the enhancement of sub-gap optical absorption in black silicon seems to correlate with the presence of S or Se in high concentration during the laser-doping, contrary to the presence of nitrogen [21]. Therefore, both BC8 NPs and the presence of chalcogen-Si bonds at interfaces can contribute to the observed sub-gap absorption enhancement. At this point, their relative importance is yet to be clarified.
- [46] R. J. Nemes *et al.*, *Phys. Rev. B* **48**, 9883 (1993)
- [47] S. J. Kim *et al.*, *J. Mater. Chem.* **20**, 331 (2010)
- [48] L. Pizzagalli *et al.*, *Phys. Rev. B* **63**, 165324 (2001)
- [49] E.-C. Cho *et al.*, *Adv. OptoEl.* **2007**, 69578 (2007)
- [50] C. Fisker *et al.*, *J. Phys. Cond. Mat.* **24**, 325803 (2012)
- [51] M. Shishkin *et al.*, *Phys. Rev. B* **75**, 235102 (2007)